

# Nickel(II) *meso*-Tetraphenyl-Homoporphyrins, -secochlorins, and -chlorophin: Control of Redox Chemistry by Macrocycle Rigidity

Colin J. Campbell, James F. Rusling, and Christian Brückner\*

Contribution from the Department of Chemistry, U-60, 55 North Eagleville Road, University of Connecticut, Storrs, Connecticut 06269

Received March 1, 2000

**Abstract:** This paper presents the first electrochemical study of Ni(II) secochlorins, chlorophin, and homoporphyrins and demonstrates the influence of macrocycle-rigidity on the site of electroreduction. Oxidations and reductions were investigated by cyclic voltammetry. The measured electrode potentials were found to be dependent on the nature of the substituents attached to the porphyrinic moiety and on the ring flexibility. The voltammetric behavior of these molecules when employed as catalysts for the electrochemical catalytic debromination of *trans*-1,2-dibromocyclohexane was used to determine whether reduction peaks were due to a metal-based (formation of catalytically active Ni(I) complexes) or ligand-based (formation of catalytically less active  $\pi$ -anion radical) reduction. The results showed that the homoporphyrins formed ligand-based reduction products. The homoporphyrins are locked into a nonplanar conformation stabilizing the small Ni(II) ion which results in their inability to accommodate the larger Ni(I) ion. In contrast, the electronically quite similar but conformationally flexible chlorin and secochlorin complexes formed Ni(I) complexes upon electrochemical reduction. Our findings shed further light on the structural features required of porphyrinic cofactors such as factor F-430 to undergo metal-centered reduction events in their catalytic cycles. The results also provide a blue-print for synthetic porphyrinic Ni(II) complexes to be utilized for electrochemical catalysis.

## Introduction

The study of the physical properties and the reactivity of synthetic porphyrinic compounds to understand the mode of action of naturally occurring porphyrinic cofactors continues to provide valuable insights. For this and other reasons, the preparation of novel porphyrins, chlorins, secochlorins (porphyrins in which one  $\beta, \beta'$ -bond is cleaved), and porphyrin-like molecules such as porphyrin isomers, expanded porphyrins, or homoporphyrins (in which at least one of the four pyrrolic units is replaced with a non-pyrrolic building block) has received enormous attention in recent years.<sup>1</sup>

Factor F-430, a Ni(II) hydrocorphin, is the prosthetic group in the enzyme methyl-coenzyme M reductase which plays a key role in the biogenesis of methane in methanogenic bacteria.<sup>2,3</sup> The active species in the catalytic cycle of the enzyme is a reduced form of F-430 containing a Ni(I) metal center.<sup>3,4</sup> These findings inspired the study of the (electrochemical) reduction of Ni(II) porphyrins and chlorins.<sup>5–10</sup>

One-electron reduction of a Ni(II) porphyrin can lead to the formation of a Ni(I) porphyrin anion, a Ni(II) porphyrin  $\pi$ -anion radical, or a species with characteristics indicating an equilibrium between the limiting resonant forms.<sup>8,11,12</sup> The factors that determine whether ligand- or metal-centered reductions occur include the nature of the macrocycle and, to a lesser degree, the experimental conditions.<sup>13,14</sup> Ni(I) has a larger ionic radius than low-spin (square-planar) Ni(II).<sup>15</sup> Consequently, macrocycles with intrinsically larger binding cavities or which can adopt conformations creating large cavities will more readily allow metal-centered reductions.<sup>6</sup> Generally, the binding cavity-size increases with increasing saturation of the porphyrinic

(1) For reviews of porphyrin and porphyrin-analog chemistry, see: (a) Asat, A.; Dolphin, D. *Chem. Rev.* **1997**, *97*, 2267–2340. (b) Sessler, J. L.; Weghorn, S. J. *Expanded, Contracted and Isomeric Porphyrins*; Pergamon: New York, 1997. (c) *The Porphyrin Handbook*; Kadish, K. M., Smith, K. M., Guillard, R., Eds.; Academic Press: San Diego, 2000; Vols. 1–10, especially Vol. 1 (Synthesis and Organic Chemistry) and Vol. 2 (Heteroporphyrins, Expanded Porphyrins and Related Macrocycles).

(2) (a) Eidsness, M. K.; Sullivan, R. J.; Schwartz, J. R.; Hartzell, P. L.; Wolfe, R. S.; Flank, A. M.; Cramer, S. P.; Scott, R. A. *J. Am. Chem. Soc.* **1986**, *108*, 3120–3121. (b) Hausinger, R. P. *Biochemistry of Nickel*; Plenum Press: New York, 1993. (c) Ermler, U.; Grabarse, W.; Shima, S.; Goubaud, M.; Thauer, R. K. *Science* **1997**, *278*, 1457–1462. (d) Telser, J. *Struct. Bonding (Berlin)* **1998**, *91*, 31–63. (e) Thauer, R. K. *Microbiology* **1998**, *144*, 2377–2406.

(3) Jaun, B.; Pfaltz, A. *J. Chem. Soc., Chem. Commun.* **1986**, 1327–1328.

(4) Telser, J.; Horng, Y.-C.; Becker, D. F.; Hoffman, B. M.; Ragsdale, S. W. *J. Am. Chem. Soc.* **2000**, *122*, 182–183.

(5) Chang, D.; Malinski, T.; Ulman, A.; Kadish, K. M. *Inorg. Chem.* **1984**, *23*, 817–824.

(6) Stolzenberg, A. M.; Stershic, M. T. *Inorg. Chem.* **1987**, *26*, 3082–3083.

(7) Stolzenberg, A. M.; Stershic, M. T. *J. Am. Chem. Soc.* **1988**, *110*, 6391–6402.

(8) Kadish, K. M.; Sazou, D.; Maiya, G. B.; Han, B. C.; Liu, Y. M.; Saoiabi, A.; Ferhat, M.; Guillard, R. *Inorg. Chem.* **1989**, *28*, 2542–2547.

(9) (a) Lexa, D.; Momenteau, M.; Mispelter, J.; Savéant, J. M. *Inorg. Chem.* **1989**, *28*, 30–35. (b) Lexa, D.; Savéant, J. M.; Su, K. B.; Wang, D. L. *J. Am. Chem. Soc.* **1987**, *109*, 6464–6470.

(10) Helvenston, M. C.; Castro, C. E. *J. Am. Chem. Soc.* **1992**, *114*, 8490–8496.

(11) Renner, M. W.; Forman, A.; Fajer, J.; Simpson, D.; Smith, K. M.; Barkigia, K. M. *Biophys. J.* **1988**, *53*, 277a.

(12) Kadish, K. M.; Franzen, M. M.; Han, B. C.; Araullo-McAdams, C.; Sazou, D. *J. Am. Chem. Soc.* **1991**, *113*, 512–517.

(13) Kadish, K. M.; van Caemelbecke, E.; Royal, G. Electrochemistry of Metalloporphyrins in Nonaqueous Media. In *The Porphyrin Handbook*; Kadish, K. M., Smith, K. M., Guillard, R., Eds.; Academic Press: San Diego, 2000; Vol. 8, pp 1–114.

(14) Kadish, K. M.; Royal, G.; van Caemelbecke, E.; Gueletti, L. Metalloporphyrins in Nonaqueous Media: Database of Redoxpotentials. In *The Porphyrin Handbook*; Kadish, K. M., Smith, K. M., Guillard, R., Eds.; Academic Press: San Diego, 2000; Vol. 9, pp 1–219.

(15) Shannon, R. D. *Acta Crystallogr.* **1976**, *A32*, 751.

macrocycle.<sup>16</sup> At the same time, the conformational flexibility of these systems also increases. Ruffling of the macrocycle results in a decrease of the central cavity-size without distortion of its square-planar coordination environment.<sup>16</sup> The combination of these effects leads to the observation that, for instance, the binding cavity size in hydroporphyrins such as OEIBCNI<sup>17</sup> can be adjusted to accommodate Ni(II) (Ni–N distance  $\sim$ 1.92 Å) and Ni(I) ions (Ni–N distance  $\sim$ 2.1 Å), evidently without requiring too much ligand reorganization energy.<sup>6</sup> In addition to the binding cavity size and conformational factors, macrocycles with intrinsic LUMOs above those of the Ni(II) d-electrons, for example porphycene, favor the formation of Ni(I) species.<sup>18</sup>

Modulation of electronic characteristics is generally brought about by proper choice of peripheral substituents on the macrocycle. However, due to steric crowding around the macrocycle, multiple peripheral substitutions may also change the conformation of the ligand, obscuring the differentiation between steric and electronic effects on the outcome of the reduction event.<sup>19</sup> Moreover, if peripheral substituents force the porphyrin into a nonplanar conformation they generally also rigidify the macrocycle and the effects of flexibility and conformation cannot be studied independently. Analogous to the reductions, observations can be made, and explanations drawn, for metal- or ligand-centered oxidation events.<sup>20</sup>

This paper presents the first electrochemical study of Ni(II) secochlorins and homoporphyrins. These porphyrinic systems provide a direct demonstration of the influence of macrocycle-rigidity on the site of electroreduction. Some Ni(II) macrocycle complexes investigated here are known to have almost identical conformations and electronic properties as expressed by their UV–visible spectra. However, a fundamental difference between these compounds is that the secochlorins are flexible while the homoporphyrins are conformationally severely restricted. We show herein that the flexible systems form Ni(I) complexes while the rigid systems form anionic Ni(II)  $\pi$ -radicals. Our findings shed further light on the structural features required of porphyrinic cofactors to undergo metal-centered reduction events

(16) (a) Kratky, C.; Waditschatka, R.; Angst, C.; Johansen, J. E.; Plaquevent, J. C.; Schreiber, J.; Eschenmoser, A. *Helv. Chim. Acta* **1985**, *68*, 1313–1337. The biological significance of nonplanar porphyrins was reviewed: (b) Scheidt, W. R.; Lee, Y. J. *Struct. Bonding (Berlin)* **1987**, *64*, 1–70. (c) Ravikanth, M.; Chandrashekar, T. K. *Struct. Bonding (Berlin)* **1995**, *82*, 105–88. (d) Shelnutz, J. A.; Song, X.-Z.; Ma, J.-G.; Jia, S.-L.; Jentzen, W.; Medforth, C. J. *J. Chem. Soc. Rev.* **1998**, *27*, 31–42.

(17) Nomenclature and abbreviations used: TBAP, tetrabutylammonium perchlorate; TBAPF<sub>6</sub>, tetrabutylammonium hexafluorophosphate; DBCH, *trans*-1,2-dibromocyclohexane; EiBCNi, octaethylbacteriochlorinato nickel(II); TPPH<sub>2</sub>, *meso*-tetraphenylporphyrin; TPPNi, *meso*-tetraphenylporphyrinato nickel(II); (OH)<sub>2</sub>TPCNI, *meso*-tetraphenyl-2,3-*cis*-dihydroxy-2,3-chlorinato nickel(II). The nomenclature of porphyrinoid systems with cleaved  $\beta,\beta'$ -bonds as well as incorporation of six-membered rings is variable. We adopted the nomenclature for homoporphyrins suggested in: Adams, K. R.; Bonnett, R.; Burke, P. J.; Salgado, A.; Asunción Vallés, M. *J. Chem. Soc., Perkin Trans. 1* **1997**, 1769–1772. And for the secochlorins we adopted the nomenclature suggested in: Flitsch, W. *Pure Appl. Chem.* **1986**, *58*, 153–160. (CHO)<sub>2</sub>TPSNI, *meso*-tetraphenyl-2,3-diformyl-2,3-secochlorinato nickel(II); (CHO)TPSNI, *meso*-tetraphenyl-2-formyl-2,3-secochlorinato nickel(II); TPCPNi, *meso*-tetraphenylchlorophinato nickel(II); (MeO)<sub>2</sub>TPMNI, *meso*-tetraphenyl-2,3-methoxy-2a-oxa-2a-homoporphyrinato nickel(II); (HO)TPMNI, *meso*-tetraphenyl-2-hydroxy-2a-oxa-2a-homoporphyrinato nickel(II); (MeO)TPMNI, *meso*-tetraphenyl-2-methoxy-2a-oxa-2a-homoporphyrinato nickel(II); (MeO)TPYNI, *meso*-tetraphenyl-2-methoxy-2a-aza-2a-homoporphyrinato nickel(II).  $E^{\circ}$  is the potential halfway between the oxidation and reduction peaks for a given electron-transfer process.

(18) Renner, M. W.; Forman, A.; Wu, W.; Chang, C. K.; Fajer, J. J. *Am. Chem. Soc.* **1989**, *111*, 8618–8621.

(19) Senge, M. O. Highly Substituted Porphyrins. In *The Porphyrin Handbook*; Kadish, K. M., Smith, K. M., Guilard, R., Eds.; Academic Press: San Diego, 2000; Vol. 9, pp 239–348.

(20) Connick, P. A.; Macor, K. A. *Inorg. Chem.* **1991**, *30*, 4654–4663.

in their catalytic cycles. Furthermore, our findings provide a blueprint for synthetic Ni(II) porphyrinic complexes to be utilized in electrochemical catalytic reactions such as those in which other transition metal macrocycles have found utility.<sup>21</sup>

The crucial role of the flexibility of the (hydro)porphyrinic ligands with respect to the outcome of biological redox events has been convincingly implied and discussed before, for instance, for the corrin of vitamin B<sub>12</sub>, the hydrocorphin of F-430, the 3,8-dioxoporphyrin of heme d<sub>1</sub> (the cofactor in dissimilatory nitrite reductase), and the isobacteriochlorin of siroheme (the cofactor of sulfite reductase).<sup>16,22</sup> However, the implications rested mostly on the comparison of macrocycles in which the conformations and electronic properties could not, as will be shown in this investigation, be varied relatively independently.

## Experimental Section

**Chemicals.**<sup>17</sup> CH<sub>2</sub>Cl<sub>2</sub> (spectrophotometric grade) was obtained from Baker and was distilled under N<sub>2</sub> from CaH<sub>2</sub> prior to use. TBAP and TBAPF<sub>6</sub> were obtained from Kodak, Acros, or Aldrich and dried under vacuum prior to use. *trans*-1,2-Dibromocyclohexane (DBCH) was obtained from Aldrich and used without further purification.

TPPH<sub>2</sub> was synthesized by the method of Adler,<sup>23</sup> and Ni(II) was inserted using standard procedures to give TPPNi.<sup>24</sup> (OH)<sub>2</sub>TPCNI,<sup>25,26</sup> (CHO)TPSNI,<sup>27</sup> (CHO)<sub>2</sub>TPSNI,<sup>25,27</sup> (MeO)<sub>2</sub>TPMNI,<sup>25</sup> and TPCPNi<sup>27</sup> were prepared as described previously. NaBH<sub>4</sub> reduction of (CHO)<sub>2</sub>TPSNI produces (HO)TPMNI, which upon methylation yields (MeO)TPMNI. (MeO)TPYNI is available by reaction of (CHO)<sub>2</sub>TPSNI with NH<sub>4</sub>OH, followed by methylation. The detailed procedures for the novel compounds will be described elsewhere.<sup>28</sup> None of the porphyrinic materials were particularly sensitive to air oxidation and all could be handled without special precautions.

**Instrumentation and Methods.** The UV–vis spectra were recorded in CH<sub>2</sub>Cl<sub>2</sub> on a Varian Cary 50 scanning spectrophotometer (wavelength accuracy  $\pm$ 0.5 nm).

Cyclic voltammetry and controlled potential electrolysis were done with BAS 100 B/W or CHI 660a electrochemistry systems. Voltammetry was carried out in an undivided three-electrode cell. The electrolyte was TBAP (0.1 M) or TBAPF<sub>6</sub> (0.1 M) dissolved in CH<sub>2</sub>Cl<sub>2</sub> and the porphyrinic analyte was present at a concentration of ca. 1 mM. For catalytic measurements, DBCH was present at a concentration of 0.03 M. The working electrode was Pt wire (cleaned by holding it in a Bunsen burner flame until red and then cooled under N<sub>2</sub>), the counter electrode was pyrolytic graphite, and the reference was an SCE. Prior to scanning, all solutions were degassed using a stream of purified N<sub>2</sub> and during experiments a blanket of N<sub>2</sub> was maintained above the solutions.

## Results

**Voltammetry with TBAP as Supporting Electrolyte.** The porphyrinic macrocycles under investigation are based on reports by Brückner et al.<sup>25–28</sup> The Ni(II) complexes of the TPP-derived porphyrinic compounds contain one  $\beta,\beta'$ -bond which is dihy-

(21) (a) Scheffold, R.; Rytz, G.; Walder, L. In *Modern Synthetic Methods*; Scheffold, R., Ed.; Wiley: New York, 1983; Vol. 3, p 355. (b) Scheffold, R.; Abrecht, S.; Orłinski, R.; Ruf, H.-R.; Stamouli, P.; Tinembart, O.; Walder, L.; Weymuth, C. *Pure Appl. Chem.* **1987**, *59*, 363–372.

(22) Barkigia, K. M.; Chantranupong, L.; Smith, K. M.; Fajer, J. *J. Am. Chem. Soc.* **1988**, *110*, 7566–7567.

(23) Adler, A. D.; Longo, F. R.; Finarelli, J. D.; Goldmacher, J.; Assour, J.; Korsakoff, L. *J. Org. Chem.* **1967**, *32*, 476.

(24) Buchler, J. W. *Synthesis and Properties of Metalloporphyrins*. In *The Porphyrins*; Dolphin, D., Ed.; Academic Press: New York, 1978; Vol. 1, Chapter 10.

(25) Brückner, C.; Steven, J.; Rettig, S. J.; Dolphin, D. *J. Org. Chem.* **1998**, *63*, 2095–2098.

(26) Brückner, C.; Dolphin, D. *Tetrahedron Lett.* **1995**, *36*, 3295–3298.

(27) Brückner, C.; Sternberg, E. D.; MacAlpine, J. K.; Rettig, S. J.; Dolphin, D. *J. Am. Chem. Soc.* **1999**, *121*, 2609–2610.

(28) Brückner, C.; Dolphin, D., and co-workers. Manuscript in preparation.

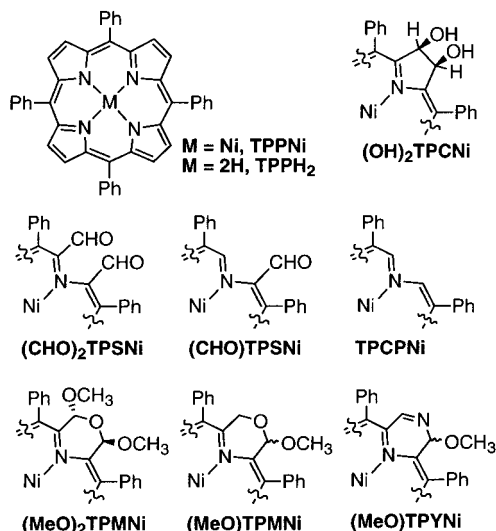


Figure 1. Structures and acronyms of the Ni-macrocycles studied.

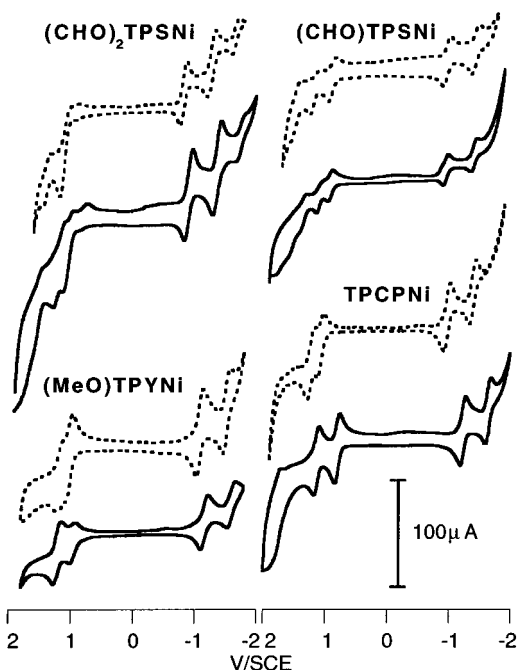


Figure 2. Representative voltammograms. Ni-complex concentration  $\sim 1$  mM, recorded on a Pt wire electrode at 0.2 V/s. Upper (dashed) trace measured in  $\text{CH}_2\text{Cl}_2/\text{TBAP}$  (0.1 M) and lower (solid) trace in  $\text{CH}_2\text{Cl}_2/\text{TBAPF}_6$  (0.1 M).

droxylated [diol chlorin  $(\text{OH})_2\text{TPCNi}$ ], cleaved [secochlorin bisaldehyde  $(\text{CHO})_2\text{TPSNI}$  and secochlorin monoaldehyde  $(\text{CHO})\text{TPSNI}$ ], or altogether removed [chlorophin  $\text{TPCPNi}$ ], or in which one pyrrolic unit was formally replaced by a six-membered ring [morpholino-type in  $(\text{MeO})_2\text{TPMNI}$  and  $(\text{MeO})\text{TPMNI}$ , pyrazine-type in  $(\text{MeO})\text{TPYNI}$ ]. The structures are shown in Figure 1.<sup>17</sup>  $\text{TPPNi}$  served as a reference compound.  $(\text{CHO})_2\text{TPSNI}$ ,  $(\text{MeO})_2\text{TPMNI}$ , and  $\text{TPCPNi}$  have been previously structurally characterized.<sup>25,27</sup>

Representative cyclic voltammograms of the compounds in Figure 1, using  $\text{CH}_2\text{Cl}_2$  with TBAP as supporting electrolyte, are given in Figure 2. Cyclic voltammograms are included in the supplementary material. Potentials as midpoints between reduction–oxidation peak pairs are summarized in Table 1. All compounds showed at least two reversible reduction peaks, negative of  $-0.8$  V vs SCE, and at least two oxidation peaks. The degree of reversibility of oxidation peaks was strongly dependent on the macrocycle structure.

$(\text{OH})_2\text{TPCNi}$  shows two reduction peaks, both of which are shifted to more negative potentials compared to the corresponding reduction peaks for the reference compound  $\text{TPPNi}$ . The first two oxidation peaks for  $(\text{OH})_2\text{TPCNi}$  are both less positive than those for  $\text{TPPNi}$ . The third and most positively positioned peak is close to the positive scan limit where solvent oxidation occurs.

The parent chlorophin  $\text{TPCPNi}$  gave a well-defined voltammogram in which there are four reversible redox pairs: two reductions and two oxidations. The first reduction appears, on the basis of peak separation and peak area ratio, to be a single electron reduction.<sup>29</sup> The second reduction peak is slightly broader but may be distorted by its proximity to the solvent reduction signal. The first oxidation peak overlaps the second oxidation peak. This feature is commonly observed for  $\text{TPPNi}$  and related systems.<sup>30</sup> Due to the overlapping nature of these two peaks it is difficult to draw any firm conclusions regarding the reversibility of the oxidation processes (see below for a discussion of the voltammograms determined in  $\text{CH}_2\text{Cl}_2$  with  $\text{TBAPF}_6$  as supporting electrolyte).

Structurally,  $(\text{CHO})\text{TPSNI}$  and  $(\text{CHO})_2\text{TPSNI}$  are formyl-substituted  $\text{TPCPNi}$ . The substituents exert an additive electronic effect on the redox behavior of the molecules. This is apparent in the shift of the first reduction potential to a more positive (easier to reduce) potential as compared to the chlorophin. The second reduction appears to be less (but still significantly) influenced by the formyl substituents.  $(\text{CHO})_2\text{TPSNI}$  exhibits a third reduction seen close to the negative scan limit. On scanning positive from 0 V one observes two distinct oxidation peaks for both formyl-substituted compounds. In both compounds, the first oxidation has a peak shape suggesting a follow-on chemical reaction that makes the electron transfer irreversible. The second peak overlaps the first and the peak separation is distorted by this overlap. There are several other signals as one scans further toward the oxidative limit but none is well-defined.

The cyclic voltammograms for the structurally related morpholino-derived homoporphyrins  $(\text{MeO})_2\text{TPMNI}$  and  $(\text{MeO})\text{TPMNI}$  are, as expected, similar. Both compounds show three oxidations and two reductions. Both reductions appear to be reversible, one-electron processes. Of the three oxidation peaks, the first is a reversible, one-electron transfer. The second (overlapping the first) has a slightly larger peak separation (greater than 120 mV) which may be the result of slower electron-transfer kinetics. The third peak is too close to the positive scan limit to make any firm conclusions based on peak separation or area ratio.

Formal replacement of the ring oxygen in  $(\text{MeO})\text{TPMNI}$  with a conjugated imine nitrogen produces the pyrazine version of this molecule,  $(\text{MeO})\text{TPYNI}$ . The electrochemical characteristics are similar to the morpholine-based macrocycle.  $(\text{MeO})\text{TPYNI}$  has a reduced first but slightly increased second reduction potential compared to  $(\text{MeO})\text{TPMNI}$ . The greatest difference between the two compounds is that the two oxidation peaks for  $(\text{MeO})\text{TPYNI}$  are significantly shifted to more positive potentials.

**Voltammetry with  $\text{TBAPF}_6$  as Supporting Electrolyte.** As previously reported for  $\text{TPPNi}$ -based systems, overlapping

(29) Bard, A. J.; Faulkner, L. R. *Electrochemical Methods*; J. Wiley & Sons: New York, 1980.

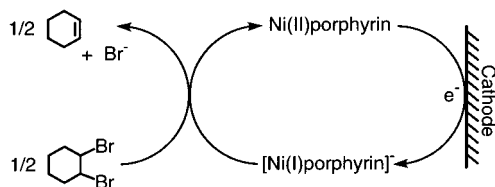
(30) (a) Kadish, K. M.; Morrison, M. M. *Inorg. Chem.* **1976**, *15*, 980–982. (b) Kadish, K. M.; Morrison, M. M.; Constant, L. A.; Dickens, L.; Davis, D. G. *J. Am. Chem. Soc.* **1976**, *98*, 8387–8390. (c) Kadish, K. M.; Morrison, M. M. *J. Am. Chem. Soc.* **1976**, *98*, 3326–3328. (d) Kadish, K. M.; Morrison, M. M. *Bioinorg. Chem.* **1977**, *7*, 107–115.



**Table 1.** Formal Potentials ( $E^{\circ'}$ )<sup>16</sup> and Potential Separation ( $\Delta E^{\circ'}$ ) for the Electron Transfer Processes Studied<sup>a</sup>

	oxidation $E^{\circ'}$ in CH <sub>2</sub> Cl <sub>2</sub> -TBAP [V/SCE]		reduction $E^{\circ'}$ in CH <sub>2</sub> Cl <sub>2</sub> -TBAP [V/SCE]		oxidation $E^{\circ'}$ in CH <sub>2</sub> Cl <sub>2</sub> -TBAPF <sub>6</sub> [V/SCE]		$\Delta E^{\circ'}$ in CH <sub>2</sub> Cl <sub>2</sub> /TBAP	$\Delta E^{\circ'}$ in CH <sub>2</sub> Cl <sub>2</sub> /TBAPF <sub>6</sub>		
<b>TPPNI</b>		1.127	-1.117		1.324	1.008	overlapping	0.316		
<b>TPCPNI</b>		1.072	-0.9680	-1.392	1.141	0.799	0.048	0.342		
<b>(OH)<sub>2</sub>TPCNI</b>	1.66	1.033	0.845	-1.170	-1.637	1.826	1.163	0.802	0.188	0.361
<b>(MeO)<sub>2</sub>TPMNI</b>	1.64	1.168	0.920	-1.084	-1.580	1.768	1.236	0.835	0.248	0.401
<b>(MeO)TPMNI</b>	1.62	1.042	0.877	-1.119	-1.517	1.618	1.123	0.825	0.165	0.298
<b>(MeO)TPYNI</b>		1.184	1.006	-1.094	-1.529		1.204	0.954	0.178	0.250
<b>(CHO)TPSNI</b>		1.361	1.104	-0.920	-1.395	1.467	1.190	0.897	0.257	0.293
<b>(CHO)<sub>2</sub>TPSNI</b>		1.472	1.118	-0.808	-1.265	-1.653	1.744	1.186	1.042	0.144

<sup>a</sup>  $\Delta E^{\circ'}$  measures the difference in potential for the first two oxidation peaks in the given solvent system.

**Scheme 1.** Scheme of the Ni(I) Porphyrin Mediated Electrochemical Debromination of DBCH

oxidation peaks can be separated by changing the supporting electrolyte from TBAP to TBAPF<sub>6</sub>.<sup>30</sup> The results for the oxidation half-wave potentials measured with this electrolyte as well as  $\Delta E^{\circ'}$  for the first two oxidation peaks in the two electrolyte systems examined are tabulated in Table 1. Analogous to precedent cases, the maximum effect on peak separation was observed for the first two oxidation peaks and the separation is most marked in the cases where the ring is most substituted with electron donating groups, i.e., in (OH)<sub>2</sub>TPCNI and (MeO)<sub>2</sub>TPMNI.

#### Determining Reduction Site through Catalytic Activity.

One-electron reduction of Ni(II) porphyrins may produce either a Ni(I) species or a Ni(II) anion  $\pi$ -radical. The Ni(I) species is capable of efficiently catalyzing the electrochemical dehalogenation of bromoalkanes (Scheme 1) by chemical catalysis (i.e. an inner-sphere electron-transfer process).<sup>9</sup> Chemical catalysis occurs by the formation of a catalyst-substrate adduct which then dissociates, eventually yielding products and the starting form of the catalyst.<sup>31</sup> The intermediacy of a chemical bond in this case allows electron transfer to occur more rapidly than in redox catalysis. In redox catalysis as carried out by a Ni(II) anion radical, an electron is transferred by an outer-sphere mechanism. Catalysis results due to the greater three-dimensional availability of electrons to the substrate when compared with a two-dimensional electrode surface. However, the rate acceleration due to inner-sphere catalysis is several orders of magnitude larger than that brought about by redox catalysis.<sup>9</sup> Thus, cyclic voltammetry performed in systems containing closely related porphyrinic Ni(II) complexes and a common substrate which can be electrocatalytically reduced (here DBCH) can be utilized to distinguish the occurrence of metal- or ligand-centered reduction events.<sup>12</sup> Electrocatalysis brought about by a Ni(I) center formed at the electrode results in the fast chemical conversion of Ni(I) to the corresponding Ni(II) species, which is then available for another cathodic reduction (Scheme 1). This results in a large current increase at the reduction peak concurrent with a minimal peak for the electrochemical back-oxidation of Ni(I) to the Ni(II) species. The voltammetric peak

(31) A alternative mechanism (halonium transfer E2 elimination) for the chemical catalysis of the reductive debromination of *vic*-dibromoalkanes has been described for Fe- and Mn-porphyrins and cannot, a priori, be excluded to operate in Ni-porphyrins as well: Lexa, D.; Savéant, J. M.; Schaefer, H. J.; Su Khac, B.; Vering, B.; Wang, D. L. *J. Am. Chem. Soc.* **1990**, *112*, 6162-6177.

**Table 2.** Peak Potentials ( $E_p$ ) and Catalytic Efficiencies ( $I_{cat}/I_D$ ) for the Electrochemical Debromination of DBCH

	$E_p$ 1st reduction [V/SCE]	$I_{cat}/I_D$ for 1st reduction	$E_p$ 2nd reduction [V/SCE]	$I_{cat}/I_D$ for 2nd reduction
<b>TPPNI</b>	-1.116	3.5		
<b>TPPH<sub>2</sub></b>	-1.010	1.1		
<b>(OH)<sub>2</sub>TPCNI</b>	-1.167	2.9		
<b>TPCPNI</b>	-1.135	2.6		
<b>(CHO)<sub>2</sub>TPSNI</b>	-0.807	1.3	-1.269	2.4
<b>(CHO)TPSNI</b>	-0.925	1.2	-1.382	2.7
<b>(MeO)<sub>2</sub>TPMNI</b>	-1.082	1.1	-1.570	1.2
<b>(MeO)TPMNI</b>	-1.517	1.4	-1.094	1.1
<b>(MeO)TPYNI</b>	-1.119	1.2	-1.529	1.3

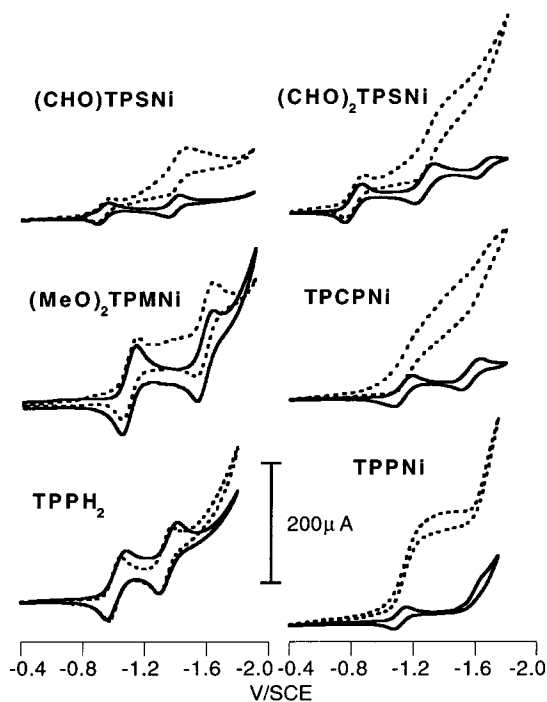


**Figure 3.** Comparison of representative voltammograms in the presence (dashed trace) and in the absence (solid trace) of DBCH (0.03M) in CH<sub>2</sub>Cl<sub>2</sub>/TBAP (0.1 M). Porphyrin concentration  $\sim$ 1 mM, scan rate 0.2 V/s.

obtained in the slower catalytic reductions, characteristic of ligand-centered  $\pi$ -anion radicals, shows a much smaller current increase under the same experimental conditions.<sup>12</sup>

We employed this technique to assess the sites of reduction of our complexes. Results in terms of catalytic efficiencies [for which the ratio of peak heights with and without DBCH ( $I_{cat}/I_D$ ) is a measure] are summarized in Table 2. Representative cyclic voltammograms with and without DBCH are shown in Figure 3. As standards with which to compare the macrocycles in question we included TPPNI, which forms TPPNI(I) upon

reduction, and **TPPH<sub>2</sub>**, which forms an anion  $\pi$ -radical. Comparison of the cyclic voltammogram of **TPPNi** with that for **TPPH<sub>2</sub>** in the absence and presence of DBCH illustrates the principle of our measurement.

**TPPNi** has two reduction peaks within the range scanned.<sup>14</sup> Upon addition of DBCH to this system, a clearly defined catalytic peak due to the mechanism outlined above can be observed. This current increase and the lack of a reverse peak are characteristic of a fast electrocatalytic reduction involving **TPPNi(I)**. The behavior of **TPPNi** contrasts well with that of free-base **TPPH<sub>2</sub>**, which also has two reduction peaks.<sup>14</sup> Upon addition of DBCH there is only a very slight increase in current at either peak and the reverse peaks are largely unaffected since the rate of the catalytic process is so slow that the reduced forms are still abundant on the reverse scan. Hence,  $I_{cat}/I_D$  is very close to unity for **TPPH<sub>2</sub>** and much smaller than this ratio determined for **TPPNi** (Table 2).

The voltammograms for **(OH)<sub>2</sub>TPCNi** and **TPCPNi** upon addition of DBCH show a response similar to that of **TPPNi**, indicating that a similarly fast inner-sphere electron transfer occurs upon generation of a Ni(I) species (Figure 3, Table 2). The voltammetric responses for **(CHO)<sub>2</sub>TPSNi** and **(CHO)-TPSNi** are different from the preceding. The first reduction peak gives only a very small current increase on addition of DBCH, and it is not until the second electron is transferred that fast catalysis can be observed.

**(MeO)<sub>2</sub>TPMNi** and its structural analogues **(MeO)TPMNi** and **(MeO)TPYNi** give voltammograms in the presence of DBCH in which there appears to be no inner-sphere catalysis at all. The more negative reduction peak gives a slightly larger catalytic peak than the first, as is predicted on increasing the reversible potential of the redox couple but nowhere near that of the inner-sphere type catalysts.<sup>32</sup>

## Discussion

**Choice of the Porphyrinic Ni(II) Complexes.** Ni(II) porphyrins are subject to a variety of out-of-plane distortions.<sup>16</sup> Hoard first noticed that since the natural cavity of porphyrins has a 2.00 Å radius, but the square-planar low-spin Ni(II)–N[pyrrole] bond distance is approximately 1.85 Å, coordination of Ni(II) to a porphyrin introduces strain into the macrocycle.<sup>33,34</sup> Due to this tendency for the metal to draw the pyrrolic nitrogens closer toward the center, a (metal-dependent) ruffling distortion of the macrocycle occurs.<sup>16,35</sup> In general, the more pronounced the distortion of the macrocycle, the shorter the Ni–N bond length. Steric clashes of peripheral substituents on the porphyrin can introduce an intrinsic ruffling of the macrocycle that may be amplified upon coordination to Ni(II). Loss of planarity of the macrocycle, however, results in loss of  $\pi$ -overlap in the macrocyclic aromatic system and it introduces distortions in the bond angles of the sp<sup>2</sup>-hybridized ring atoms. The equilibrium structure finds a balance between the competing forces.<sup>36</sup> With

increasing saturation of the macrocycle, the loss of  $\pi$ -overlap upon distortion from planarity becomes less severe. This leads to a larger out-of-plane flexibility of the hydrophorphyric macrocycles, and a number of examples have been provided.<sup>16</sup>

Breaking the structural integrity of the Ni(II) porphyrin macrocycle by complete removal of one  $\beta, \beta'$ -bond (as in **TPCPNi**) results in a severely nonplanar conformation with average Ni–N bond distances of 1.912(3) Å (RMS of the C<sub>18</sub>N<sub>4</sub>-Ni mean plane = 0.368 Å).<sup>27</sup> This illustrates the intrinsic flexibility of the macrocycle. The compound **(CHO)<sub>2</sub>TPSNi** can be regarded as the bis-formyl-substituted chlorophin **TPCPNi** and its ruffled conformation has also been determined.<sup>27</sup> The formyl substituents amplify the ruffling mode, resulting in average Ni–N bond distances of 1.892(3) Å (RMS of the C<sub>18</sub>N<sub>4</sub>-Ni mean plane = 0.465 Å). The flexibility of these systems is also reflected in the <sup>1</sup>H NMR spectrum of **(CHO)<sub>2</sub>TPSNi** which features temperature-dependent broadening of some peaks which we attribute to dynamic conformational effects. The electronic structure of the formyl compounds is significantly different from that of the chlorophin as illustrated by their UV–vis spectra.<sup>27</sup> The secochlorin monoaldehyde **(CHO)TPSNi** ( $\lambda_{max}$  = 678 nm) lies electronically between **(CHO)<sub>2</sub>TPSNi** ( $\lambda_{max}$  = 686 nm) and **TPCPNi** ( $\lambda_{max}$  = 612 nm) and its conformation can be extrapolated from the two aforementioned compounds.

Conformation of the homoporphyrin **(MeO)<sub>2</sub>TPMNi** is nearly identical with that of **(CHO)<sub>2</sub>TPSNi** (median Ni–N bond length for **(CHO)<sub>2</sub>TPSNi** of 1.895(3) Å, RMS of the C<sub>18</sub>N<sub>4</sub>-Ni mean plane = 0.468 Å).<sup>25</sup> The absence of the conjugated formyl groups, however, renders the homoporphyrin ( $\lambda_{max}$  = 640 nm) to be electronically significantly different from the bisaldehyde. Most importantly, the presence of the fused six-membered ring is believed to lock the macrocycle into one rigid conformation since expansion (or contraction) of the core by means of a reduction of the degree of nonplanarity of the macrocycle leads to an energetically unfavorable flattening of the fused morpholine-type ring (Figure 4 B,C). Moreover, the steric interaction of the substituents on the morpholine unit with the adjacent *meso*-phenyl groups introduces a further rigidifying effect (Figure 4A shows the spatial relationship between the substituents, here hydrogen atoms, and the phenyl groups). While it is theoretically possible that an as yet unobserved mode of distortion could be adopted by the macrocycle so as to allow for a core widening without a flattening of the fused six-membered ring, it seems unlikely. The rigidity of the macrocycle also implies that interconversion between the two chiral (point group C<sub>2</sub>) conformations via a planar species (Figure 4C) is made impossible (Figure 4, B to D conversion), fostering the hope that the enantiomeric conformers could be separated.<sup>37</sup>

The compound **(MeO)TPMNi** ( $\lambda_{max}$  = 640 nm) was included in this study to test the rigidifying effect of the methoxy substituents on the morpholino ring in the otherwise electronically very similar (as judged by a comparison of their identical  $\lambda_{max}$ ) macrocycles **(MeO)TPMNi** and **(MeO)<sub>2</sub>TPMNi**. Following the same rationale as outlined above, the pyrazine-derived homoporphyrin **(MeO)TPYNi** is also believed to be a rigid macrocycle. Molecular modeling studies indicate that its conformation differs little from that of **(MeO)TPMNi**.<sup>38</sup> The presence of the imine group which is in conjugation with the 18 $\pi$ -system of the macrocycle, however, modulates the electron density of this compound ( $\lambda_{max}$  = 620 nm) as compared to that of the morpholino-derived homoporphyrins.

(32) Andrieux, C. P.; Dumas-Bouchiat, J.-M.; Savéant, J.-M. *J. Electroanal. Chem.* **1978**, *87*, 39–53.

(33) Hoard, J. L. *Science* **1971**, *174*, 1295.

(34) (a) Henrick, K.; Tasker, P. A.; Lindoy, L. F. *Prog. Inorg. Chem.* **1985**, *33*, 1–58. (b) Ni–N bond distance in bis(*meso*-phenyl)dipyrrinato Ni(II) 1.879(2) Å: Brückner, C.; Karunaratne, V.; Rettig, S. J.; Dolphin, D. *Can. J. Chem.* **1996**, *27*, 2182–2193.

(35) Sparks, L. D.; Medforth, C. J.; Park, M. S.; Chamberlain, J. R.; Ondrias, M. R.; Senge, M. O.; Smith, K. M.; Shelnutz, J. A. *J. Am. Chem. Soc.* **1993**, *115*, 581–592.

(36) This balance is a delicate one. OEPNi, for instance, crystallizes in planar and ruffled polymorphs: (a) Cullen, D. L.; Meyer, E. F., Jr. *J. Am. Chem. Soc.* **1974**, *96*, 2095–2102. (b) Meyer, E. F., Jr. *Acta Crystallogr., Sect. B* **1972**, *B28*, 2162–2167. (c) Brennan, T. D.; Scheidt, W. R.; Shelnutz, J. A. *J. Am. Chem. Soc.* **1988**, *110*, 3919–3924.

(37) Furusho, Y.; Kimura, T.; Mizuno, Y.; Aida, T. *J. Am. Chem. Soc.* **1997**, *119*, 5267–5268.

(38) CACHE V4.02; Oxford Molecular Group: Oxford, 1999; MM3 force field.

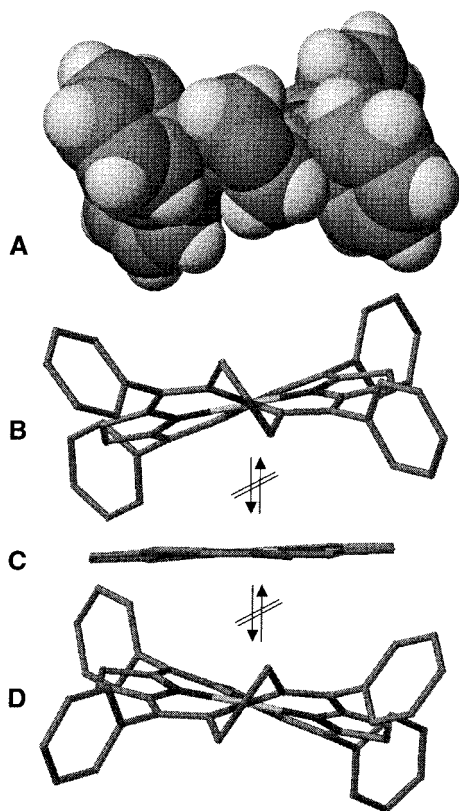


**Figure 4.** Space filling (A, van der Waals radius) and wire frame model (B–D) of homoporphyrin conformation and theoretical interconversion of the two enantiomers. Minimized molecular model (MM3)<sup>34</sup> based on X-ray crystallographically determined atomic coordinates for (MeO)<sub>2</sub>TPMNI.<sup>23</sup>

#### Determining Reduction Site Through Catalytic Activity.

The results tabulated in Table 2 and Figure 3 unambiguously show that (OH)<sub>2</sub>TPCNI and TPCPNI have a catalytic behavior characteristic of inner-sphere electron-transfer catalysis. Thus, Ni(I) species were formed upon reduction.

The two cases in which (electron withdrawing) formyl groups have been attached to the TPCPNI system [(CHO)<sub>2</sub>TPSCNI and (CHO)TPSCNI] also show catalytic activity but not until the potential has been increased to the value of the second reduction peak. One can conclude that the first electron transferred resides on the ligand (and is possibly largely localized at the formyl groups) and only upon the transfer of a second electron does generation of the catalytic Ni(I) species occur. Bulk electrolysis of (CHO)<sub>2</sub>TPSCNI at the potential of the first reduction peak (−810 mV) produced (OH)<sub>2</sub>TPCNI as the major product, in addition to a small amount of a number of unidentified products. (OH)<sub>2</sub>TPCNI is the pinacol reduction product of the bisaldehyde, indicating that, indeed, the first reduction peak is ligand (formyl group) centered. The trans-isomer of (OH)<sub>2</sub>TPCNI would also have been an expected product but it could not be identified.

It is surprising when comparing the electronic and conformational similarities of TPCPNI and (OH)<sub>2</sub>TPCNI with those of the homoporphyrins that none of the homoporphyrins showed a significant catalytic activity upon reduction, indicating the absence of any Ni(I) species formed. What differentiates the homoporphyrins from regular chlorins, porphyrins, or secoclorins? What makes the formation of a Ni(I) species evidently impossible?

We propose that the observed behavior can be attributed solely to the rigidity of the homoporphyrins. As known from

the X-ray crystal structures, the Ni–N bond length in these systems is close to ideal for Ni(II).<sup>25,27,34</sup> The core must widen significantly to accommodate a Ni(I) center. This, though, is made sterically difficult or impossible by the fused six-membered ring. Thus, the coordination environment is unfavorable with regard to the stabilization of Ni(I) and, consequently, the ligand-centered reduction event becomes energetically more favorable.

To our knowledge, this is the first example in which the effects of the rigidity of a porphyrinic molecule on the outcome of an electroreduction are made clear. Our interpretation is consistent with and complements other related findings.<sup>39</sup> For example, Weiss and co-workers demonstrated the mutual dependence of ligand conformation and the size of the central metal:<sup>40</sup> axial ligand-induced switching of a (relatively small) low-spin metal center to a (relatively large) high-spin center led to a flattening of the macrocycle. Fukuzumi, Guillard, Kadish, and co-workers measured the electron-transfer rates for the reduction of Mn(III) to Mn(II) porphyrins in a series of planar and nonplanar porphyrins.<sup>41</sup> They found that the nonplanar porphyrins which, due to a decreased central cavity size accommodate Mn(III) better than the larger Mn(II), have a higher reorganization energy barrier for reduction, resulting in, as also predicted by the Marcus equation, slower electron-transfer rates.

**Cyclic Voltammetry.** The cyclic voltammogram for (OH)<sub>2</sub>TPCNI is as expected for a Ni(II) chlorin. (OH)<sub>2</sub>TPCNI is harder to reduce and easier to oxidize than the corresponding porphyrin complex TPPNI, reflecting the raised HOMO and LUMO of the chromophore.<sup>42</sup> TPCPNI behaves as expected when compared to (OH)<sub>2</sub>TPCNI. One may explain the lower oxidation and higher reduction potential measured for (OH)<sub>2</sub>TPCNI as compared to those for TPCPNI with the inductive effect of the electron-releasing −CHOH moiety. In contrast to the diol, TPCPNI is not, as one may expect based on their identical chromophores and identical UV–vis spectra, harder to reduce than TPPNI. This we attribute to its flexibility, allowing for the formation of a Ni(I) species without having to overcome a large rearrangement energy.

(CHO)TPSCNI and (CHO)<sub>2</sub>TPSCNI, when regarded as formyl-substituted TPCPNI (and knowing their very similar conformations), show predictable substituent effects.<sup>43</sup> The first reduction potential of (CHO)TPSCNI is lowered compared to that of TPCPNI and oxidation of the formyl-substituted systems is made harder. The irreversible character of the oxidation peaks indicates that follow-on chemical reaction occurs upon oxidation. Indeed, thin-layer chromatography of the reaction mixture made by bulk electrolysis of (CHO)<sub>2</sub>TPSCNI at the potential of the first oxidation peak resulted in the decomposition of (CHO)<sub>2</sub>TPSCNI and the appearance of several, as yet unidentified, porphyrinic compounds.

(39) Kadish, K. M.; Van Caemelbecke, E.; D'Souza, F.; Medforth, C. J.; Smith, K. M.; Tabard, A.; Guillard, R. *Inorg. Chem.* **1995**, *34*, 2984–2989.

(40) Duval, H.; Bulach, V.; Fischer, J.; Weiss, R. *Inorg. Chem.* **1999**, *38*, 5495–5501.

(41) Fukuzumi, S.; Nakanishi, I.; Barbe, J.-M.; Guillard, R.; Van Caemelbecke, E.; Guo, N.; Kadish, K. M. *Angew. Chem., Int. Ed. Engl.* **1999**, *38*, 964–966.

(42) Fayer, J. *Chem. Ind.* **1991**, 869–873. The MOs of nonplanar porphyrins have been calculated as well, for instance: (a) Barkigia, K. M.; Renner, M. W.; Furenliid, L. R.; Medforth, C. J.; Smith, K. M.; Fajer, J. *J. Am. Chem. Soc.* **1993**, *115*, 3627–3635. (b) For a DFT-SQM force field for Ni(II) porphine see: Kozłowski, P. M.; Rush, T. S., III; Jarzecki, A. A.; Zgierski, M. Z.; Chase, B.; Piffat, C.; Ye, B.-H.; Li, X.-Y.; Pulay, P.; Spiro, T. *J. Phys. Chem. A* **1999**, *103*, 1357–1366.

(43) Chen, H. L.; Ellis, P. E., Jr.; Wijesekera, T.; Hagan, T. E.; Groh, S. E.; Lyons, J. E.; Ridge, D. P. *J. Am. Chem. Soc.* **1996**, *116*, 1086–1089.



The range of homoporphyrins investigated did not show shifts in peak potentials that were predictable from electronic effects alone. When compared to **(MeO)TPMNI**, addition of a second MeO substituent in **(MeO)<sub>2</sub>TPMNI** resulted in an easier first reduction but harder second reduction. As shown above, both reductions are ligand centered. Given that both compounds have the same conformation, this observation can be interpreted in terms of a rigidification of the macrocycle by means of steric crowding rather than being electronically induced. This stiffening of the macrocycle makes a (ligand- or metal-based) reduction harder since neither a reduced (larger) metal center can be accommodated nor is a rigid nonplanar  $\pi$ -system very well set up to delocalize any charge.

Both morpholino-based homoporphyrins exhibit three oxidations. The peaks for **(MeO)<sub>2</sub>TPMNI** shifted toward higher potentials as compared to **(MeO)TPMNI**. The separation of the first two oxidation potentials has been correlated with the electron donating ability of substituents in **TPPNI**-derived systems: increasing the electron-donor ability increased the separation of the oxidation peaks.<sup>30</sup> As expected, in  $\text{CH}_2\text{Cl}_2/\text{TBAPF}_6$ , we found the largest separation for **(MeO)<sub>2</sub>TPMNI** followed by **(MeO)TPMNI**. One can infer that with increasing substitution the rigidity of the system is likely to increase (compare to Figure 4). Again, increased rigidity allows neither for a better accommodation of a small Ni(III) center by increase of the ruffling, nor does it favor delocalization of the  $\pi$ -cation radical.

The presence of an electron-withdrawing imine nitrogen in **(MeO)TPYNI** affects the ligand-centered (vide infra) reduction half wave potentials little when compared to **(MeO)TPMNI** but the oxidation potentials are significantly higher. Evidently, the imine group lowers the LUMO little while lowering the HOMO significantly compared to **(MeO)TPMNI**. Consistent with this picture,  $\lambda_{\text{max}}$  of this system is shifted 20 nm hypsochromically compared to that of **(MeO)TPMNI**.

## Conclusion

The flexibility of a nonplanar porphyrinic ligand can influence an electron-transfer reaction, such as a reduction, in two ways. First, increasing the rigidity of the ligand can change the site of electron localization from the metal center to the ligand due to the inability of the more rigid ligands, in this case the homoporphyrins, to increase their cavity size to accommodate the larger Ni(I) ion. Second, within the homoporphyrin series, the more rigidified but conformational identical systems have more negative reduction potentials due to the decreased ability of the rigid systems to delocalize the anionic charge.

Although the effect of nonplanarity on the position of the frontier orbitals in nonplanar porphyrinic systems has been the subject of a number of investigations, the influence of the flexibility of these systems, while often implied, is less well studied. With the availability of the structurally characterized Ni(II) complexes of the *meso*-tetraphenylporphyrin-derived series of secochlorins, homoporphyrins, and chlorophin which possess similar conformations but different degrees of flexibility, an appropriate model was found with which to study the influence of flexibility on the redox potentials and site of reduction. Perhaps these findings will help to delineate the modes of action of naturally occurring nonplanar porphyrinic systems involved in electron-transfer reactions and to help design efficient catalysts for electrochemical systems.

**Acknowledgment.** C.J.C. and J.F.R. are grateful to NSF for financial support (Grant Nos. CTS-9632391 and 9982854). C.B. thanks the UConn Research Foundation for financial assistance.

**Supporting Information Available:** Set of all cyclic voltammograms for all compounds studied (PDF). This material is available free of charge via the Internet at <http://pubs.acs.org>.

JA000749+